

Gradual cross-over from sub-diffusion to normal-diffusion: a many-body volume-exclusion effect of protein surface water

Pan Tan^{1,2#}, Yihao Liang^{1,2#}, Qin Xu³, Eugene Mamontov⁴, Jinglai Li^{2,5}, Xiangjun Xing^{1,6*} and Liang Hong^{1,2*}

¹ School of Physics and Astronomy, Shanghai Jiao Tong University, Shanghai 200240, China.

² Institute of Natural Sciences, Shanghai Jiao Tong University, Shanghai 200240, China

³ State Key Laboratory of Microbial Metabolism and School of Life Sciences and Biotechnology, Shanghai Jiao Tong University, Shanghai 200240, China

⁴ Spallation Neutron Source, Oak Ridge National Laboratory, Oak Ridge, TN 37831, USA

⁵ School of Mathematical Science, Shanghai Jiao Tong University, Shanghai 200240, China.

⁶ Collaborative Innovation Center of Advanced Microstructures, Nanjing 210093, China

Abstract

Dynamics of hydration water is essential for the functionality of bio macromolecules. Previous studies have demonstrated that water molecules exhibit sub diffusion on the surface of bio-macromolecules; yet the microscopic mechanism remains vague. Here, by performing neutron scattering, molecular dynamics simulations and analytic modelling on hydrated perdeuterated protein powders, we found that water molecules jump randomly between trapping sites on protein surfaces, whose waiting times obey a broad distribution, resulting in sub-diffusion. Moreover, the sub diffusive exponent gradually increases with observation time towards normal diffusion due to a many-body volume-exclusion effect.

Introduction

Water is the solvent of life, playing a crucial role in determining the native structure, dynamics and function of biological macromolecules [1-5]. The diffusive motions of water molecules not only aid the transportation of the function-required essential ingredients, e.g., protons, ions and substrates across membranes and into the catalytic site of enzymes [1,6,7], but also render internal flexibility to the bio macromolecules. This flexibility is likely to be crucial for the bio-function, as it is absent when the bio macromolecules are dehydrated [1-3,8]. On the other hand, as an active solute, the bio macromolecule will significantly alter the structure and dynamics of the hydration water molecules surrounding it [9-13]. Both experiments and simulations showed that the diffusive motion of the hydration water on the surface of various bio macromolecules: DNA [10], RNA [14], Proteins [11], and lipid membranes [12], are significantly retarded as compared to bulk water, and presents an anomalous sub diffusion [11,12,15,16]. This sub-diffusive motion is characterized by a fractional power-law dependence on time of the mean square atomic displacement (MSD), i.e., $\langle X^2(\Delta t) \rangle \sim t^\beta$, with $\beta < 1$ [11,12,15,16]. Two plausible physical pictures have been proposed to explain sub diffusion of hydration water [17-19]: spatial disorder, i.e., the

rough surface of the bio macromolecules forms a fractal, percolated network to hinder the diffusion of water molecules; or temporal disorder, i.e., water molecules jump between traps on the surface of the bio-macromolecules with a broad distribution of trapping times. Due to lack of microscopic evidences, however, the precise physical mechanism remains largely unclear [17,18].

In this work, we studied the diffusive dynamics of surface water on hydrated perdeuterated green fluorescent protein (GFP) and Cytochrome P450 (CYP) at physiological conditions by combining neutron scattering experiments with molecular dynamics (MD) simulations and analytic modeling. We showed that the dynamics of hydration water is sub-diffusive, and the sub-diffusion exponent gradually increases over the observation time. By analyzing the MD trajectories of individual water molecules, we directly observed the discrete trapping events of the water molecules on the protein surface, and found that the associated trapping times obey a broad distribution, leading to the sub diffusion. Moreover, we found that deep trapping sites are mostly occupied and thus water molecules prefer to jump among shallow traps, rendering a gradual increase of sub-diffusive power law with the observation time, towards normal diffusion. Finally, a lattice toy model, Many-Body Continuous Time Random Walk, is developed to provide a complete, quantitative description of all the relevant features of diffusive dynamics of the hydration water.

Results and discussions

Neutron scattering directly probes the fluctuation of nuclear position and is highly sensitive to hydrogen atoms. Hence, it is a powerful tool for the study of diffusive motion of water in variety of environments, from porous silica to carbon nanotube or the surface of bio macromolecules [11,16,20,21]. Here, the neutron scattering experiments were performed at 280 K on both perdeuterated GFP and CYP (see Figs. 1A and B) at hydration level of 0.4 g water/g protein, using the backscattering spectrometer (BASIS) at oak ridge national lab (ORNL) [22]. This hydration level corresponds roughly to one single layer of water molecules covering the protein surfaces [1]. The perdeuterated proteins hydrated by H₂O are the experimental key here to suppress the contribution from protein hydrogen atoms to the neutron signals, and the measured neutron data thus dominantly reflect the dynamics of hydration water. For quantitative comparison, all-atom MD simulations were performed at the same hydration level and temperature as experiments. Details of experimental and MD protocol are provided in the Supporting Information (SI).

The experimentally measured quantity is the so-called dynamic structure factor $S(q,\nu)$, which presents the amplitude-weighted distribution of the dynamic modes in the sample over frequency at a given wave vector, q . It is informative to represent neutron scattering spectra as the imaginary part of the dynamic susceptibility, $\chi''(q,\nu) = S(q,\nu)/n_B(\nu)$, $n_B(\nu)$ being the Bose factor $n_B(\nu) = [\exp(\frac{h\nu}{kT}) - 1]^{-1}$. The physical significance of $\chi''(q,\nu)$ is that it highlights the quasi-elastic components in the neutron signals and feature relaxation processes on different time scales as distinct

peaks with associated characteristic relaxation times as $t_c=1/(2\pi \nu_{\text{peak}})$ [15,23,24].

Figs. 2A and B present experimental and MD-derived susceptibility spectra χ'' for hydration water on CYP and on GFP at various q , respectively, which are in good mutual agreement. The Cole-Cole distribution function [15,23] (see Eq. (S2) in SI) is applied to model both the experimental and MD-derived susceptibility spectra χ'' , providing the value of characteristic relaxation time, t_c at a given q , i.e., roughly the time for water molecules to diffuse a distance of value $\sim 2\pi/q$. The q -dependence of the resulting t_c is presented in Fig. 2C on a double logarithmic scale for both experimental and simulation systems, which are again in quantitative agreement, validating the simulation systems on the time scales from 10 ps to 1 ns . The wave vectors measured experimentally (Fig. 2C) range from 0.7 to 1.7 \AA^{-1} , corresponding to a spatial range of 4 \AA – 1 nm. Different power-law dependences, $t_c \propto q^{-n}$, are observed for hydration and bulk water. For hydration water on either CYP or GFP, n is found to be 2.5 ± 0.1 , indicating a sub-diffusive motion $\langle X^2(\Delta t) \rangle \sim t^\beta$ with $\beta = 2/n = 0.8 \pm 0.03$ in the time window probed (10 ps to 1 ns). In contrast, a normal diffusion is observed in bulk water, which corresponds to $n=2$, $\beta=1$ (Fig. 2C). Fig. 2D presents the MD-derived $\langle X^2(\Delta t) \rangle$ for both hydration water and bulk water in the same time window as probed experimentally, an effective power-law fit provides, $\beta=0.8$ and $\beta=1$, respectively, confirming the values derived from the neutron susceptibility spectra. The value of β for the protein hydration water obtained in the present work is in quantitative agreement with the values reported in early neutron experiments and MD simulations [11,15,17-19].

Moreover, the characteristic relaxation time t_c for hydration water is found to be about an order magnitude longer than that of bulk water, which is in agreement with earlier neutron results [11,15,23], indicating the diffusion of hydration water is highly retarded near the protein surfaces. All these results are likely to be quite general for hydration water on proteins, since the two proteins studied here differ considerably in both secondary and tertiary structures (Figs. 1A and B): whereas GFP consists of mostly of β -sheets wrapped into a barrel-like structure, CYP consists of comparable amounts of β -sheets and α -helices and forms three closely-packed domains [25].

Two distinct physical pictures have been previously proposed to heuristically understand the sub diffusion of hydration water, which may be conveniently called the scenario of *spatial disorder* and that of *temporal disorder* [17-19]. In the scenario of spatial disorder, the protein surfaces have rough and fractal structures, which slow down the dynamics of hydration water and lead to sub diffusion. Mathematically, $\langle X^2(\Delta t) \rangle$ of diffusing molecules scales as t to the power of d_f/d_s , where d_f is the fractal dimension of the network of the jump motions, and d_s is the spectral dimension and is related to the connectivity of the network [17,18]. In the alternative scenario of temporal disorder, water molecules are assumed to jump stochastically between many trapping sites with a broad distribution of **trapping times**, which is defined as the time a molecule spends at a trapping site before its next jumping trial. In the simple toy model called *Continuous Time Random Walk* (CTRW), the distribution of trapping time is assumed to be power-law like with the divergent expectation of the mean value: $P(\tau) \sim$

$\tau^{-(1+\mu)}$, $0 < \mu < 1$. The exponent of the sub diffusion is thus fully determined by μ as $\langle X^2(\Delta t) \rangle \sim t^\mu$ [17,18,26]. We note however these two scenarios are NOT necessary to be mutually exclusive in principle. Hybrid theories involving both mechanisms have been proposed in literature, e.g., to explain the sub-diffusive protein internal dynamics [27].

An important difference between the two physical pictures is that walking steps for a single particle are expected to be strongly correlated over the entire jumping progress in the scenario of spatial disorder, because of the intrinsic long range correlation in the percolated fractal network of the jump motions, while no such correlation is expected in the scenario of temporal disorder [26,28].

To explore the microscopic mechanism of the sub-diffusive dynamics (Fig. 2), we analyze quantitatively the MD trajectories of each water molecule on the protein surface. Fig. 3A is a projection of the MD trajectory of the oxygen atom of one selected water molecule on CYP recorded continuously at every 100 picoseconds over 100 nanoseconds, and a video displaying this trajectory is presented in SI. More examples of such projected MD trajectory of water molecules on CYP and GFP are presented in Fig. S2 (SI). Upon observation of these trajectories, it becomes clear that the water dynamics consists of two modes: rattling within one trapping site (basin) at short time scales and jumping over to neighboring traps at longer time scales. The typical jump distance is about 2-3Å, even though longer jumps do exist. (More statistical analysis on jump distances is displayed in Table ST1 in SI.) This provides a strong support for the scenario of temporal disorder. Moreover, the typical size of trapping basins is about 1~2Å. It is very unlikely that two water molecules occupy the same basin at the same time, as the inter water molecule distance is about 3 Å as evident by the radial distribution function of hydration water molecules (Fig. S3 in SI).

For statistical analysis, the trajectories of all water molecules in the simulation of hydrated CYP were projected similarly as Fig. 3A, all trapping events were identified, and all jumping displacements \vec{s}_i were determined. The correlation function between distinct jump displacements for a given water molecule is defined as [26,28]

$$C(k) = \langle \vec{s}_i * \vec{s}_{i+k} \rangle, \quad (1)$$

where \vec{s}_i and \vec{s}_{i+k} are, respectively, the displacement vectors for the i -th and $(i+k)$ -th jumps of the molecule, and the bracket indicates ensemble average over all the hydration water molecules, and the results are presented in Fig. 3B for CYP and in Fig. S4B for GFP. Virtually zero correlation is observed, which clearly excludes the scenario of spatial disorder.

Using MD trajectories, we also analyzed the distribution of **waiting times** τ_w , defined as the time a water molecule spends at a site before jumping out. As shown in Figs. 4A and 5A, the distribution $P(\tau_w)$ is very broad. Analyses of protein surface structures indicate that residues with charges and local concave geometry tend to have longer waiting time. Details are discussed in SI.10. It is also evident from Figs. 4A and 5A that the log-log plot of $P(\tau_w)$ continuously bends downwards as τ_w increases, and the effective slope steadily increases from 0.3 to 1.3 over the observation time from 10

ps to 100 ns. Concomitantly, MD-derived $\langle X^2(\Delta t) \rangle$ exhibits a cross-over from sub diffusion to normal diffusion (Figs. 4B and 5B) with the observation time, and the effective power law, β , changes gradually from ~ 0.75 to ~ 0.95 over the time window studied (see Figs. 4C and 5C). A simple CTRW model is clearly incapable of explaining these behaviors. It is of importance to note that there is no significant time-window where the exponent stays constant, and the exponent, 0.8, obtained in Fig. 2D is an effective fit averaging over the experimental time window from 10 ps to 1ns.

The model CTRW treats all water molecules on the protein surface independently, i.e., it ignores interaction between neighboring water molecules. At the hydration level of $h=0.4$ studied here, about 48% of the trapping sites on CYP surface and 46% on the GFP surface are covered by water. (This occupancy rate is estimated as the ratio between the number of water molecules and that of trapping sites on the protein surface discovered in MD.) Consequently, there would be a substantial probability that a molecule jumps into an occupied site if it follows CTRW model. This is clearly unphysical, since the trapping sites (Fig. 3A) are not large enough to hold two water molecules. On the other hand, a deep trap is most likely occupied for long time by one given molecule, and therefore inaccessible to jumping molecules. Hence, water molecules should preferentially jump to shallow traps, and therefore effectively diffuse faster.

Model and analyses

To capture these nontrivial consequences of volume-exclusion interaction, we modify and generalize the CTRW model. We require that each site can hold at most one molecule, and assume that a fraction η of sites are occupied. As in the CTRW model, each trapping site is characterized by an *intrinsic trapping time* (ITT), denoted as τ , whose physical significance is *the average time* that a particle stays on this site, *if all other sites are empty*. The probability distribution of τ follow a power law $f(\tau) = \mu \tau_0^\mu \tau^{-1-\mu}$. A water molecule at a site with τ tries to jump to a randomly selected site with probability $1/\tau$ per unit time, and the jump is successful only if the target site is empty. If the target site is already occupied, the jumping molecule is bounced back to the original site. We call the modified model the **Many-Body Continuous Time Random Walk** (MB-CTRW) model.

We note that τ is an intrinsic property of a trapping site, and is different from the *waiting time* τ_w observed in MD at a given hydration level. The latter depends not only on the potential well of the trapping site, but also on the occupancy rate of neighboring traps. Given the distribution of τ , the probability distribution of waiting time τ_w can be calculated using the *mean-field approximation*. With technical details relegated to SI, the final result is

$$P(\tau_w) = \mu \tau_0^\mu (1 - \eta) \int_{\tau_0}^{\infty} d\tau \frac{\tau^{-2-\mu}}{1-\eta+C\tau} e^{-\frac{\tau_w(1-\eta)}{\tau}}, \quad (2)$$

where C is a function of τ_0 , μ , and η , defined in Eq. (S7) in SI. The values of these three parameters are determined by fitting Eq. (2) to MD-derived distribution of waiting

time. The key result of MB-CTRW is the gradual change of $P(\tau_w)$, because the many-body volume-exclusion effect will enhance the sampling rates of shallow trapping sites over the deep ones, which will gradually modify $P(\tau_w)$ to continuously bend downwards. This is the essential feature of $P(\tau_w)$ found in MD. As shown in Figs. 4A and 5A, a remarkable agreement of $P(\tau_w)$ between MB-CTRW and MD simulation for hydration waters on both CYP and GFP is achieved by choosing proper values of τ_0 , μ and η . The values of η resulting from fittings are 0.52 and 0.49 for hydration waters on CYP and GFP, respectively, very close to the value directly estimated from MD, which provides a strong support for the plausibility of our model. We also use Eq. (2) to simulate $\langle X^2(\Delta t) \rangle$ (see details in SI), and find remarkable agreement with MD results, as shown in Figs. 4C, 4D, 5C and 5D for hydration waters on CYP and GFP, quantitatively validating our model, MB-CTRW.

Conclusion

We have developed a comprehensive and compelling physical picture for the diffusion of hydration water on protein surfaces. We have demonstrated the existence of trapping basins for hydration water, and have shown that the sub-diffusive motion arises from the broad distribution of trapping times. The deep trapping sites are however mostly occupied, and thus diffusing water molecules preferentially jump to shallow sites. This many-body volume-exclusion interaction leads to biased sampling of trapping time, and resulting in continuous increase of the effective diffusion exponent β as observation time, i.e., gradual crossover from sub diffusion to normal diffusion. All these features are accurately captured by our mean field lattice toy model (Many-Body Continuous Time Random Walk) with remarkable precision.

It has been widely demonstrated that dynamics of water is strongly coupled to that of the enclosed protein molecule, e.g., through hydrogen bonds [24,29]. The mobility of water can thus be passed on to the protein through such coupling, and then influences or even controls the dynamical behaviors of functional importance, such as the fluctuation rate of the protein among different enzymatic states and the migration rate of ligands in and out of the catalytic pocket of the protein molecule, etc [30]. The present work shows that the many-body volume-exclusion effect makes water molecules to jump preferentially among shallow sites as the deep ones are likely to be occupied, and thus effectively diffuse faster. The resulting greater mobility in water can be eventually delivered to the enclosed protein molecule to gain sufficient flexibility required for its function. This might provide a mechanism to explain why certain hydration (about 20% in weight) is required for enzymes to present appreciable anharmonic dynamics and bioactivity [1] as such many body effect will be insufficient when the hydration level is too low.

Acknowledgements:

The authors acknowledge NSF China 11674217, 11504231, 31400707, 31770772 and 31630002 for financial support, and the Center for High Performance Computing

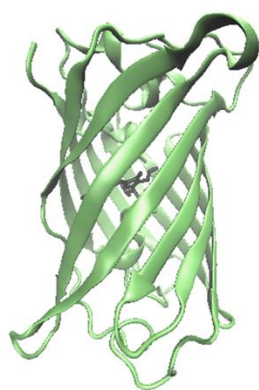
at Shanghai Jiao Tong University for computing resources. The authors also thank for Dr. Benjamin Lindner for discussion about the manuscript, Miss Keyi Wu for discussion about CTRW and Mr. Zhuo Liu for assistance on the neutron scattering experiment at Oak Ridge National Lab. The neutron scattering experiment on BASIS (SNS, ORNL) was supported by the Scientific User Facilities Division, Office of Basic Energy Sciences, U.S. Department of Energy. Oak Ridge National Laboratory is managed by UT-Battelle, LLC, for the U. S. DOE under Contract DE-AC05-00OR22725.

Author contributions:

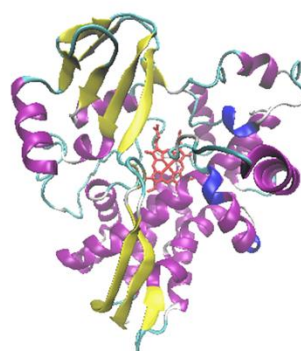
#All authors contributing equally to this work.

*Authors to whom correspondence should be addressed: xxing@sjtu.edu.cn; hongl3liang@sjtu.edu.cn.

Pan Tan did the molecular dynamics simulation and analyzed the experimental and simulation results. Yihao Liang built up the theoretical model and carried out analysis. Qin Xu and Jinglai Li wrote the manuscript. Xiangjun Xing and Liang Hong conceived the research and wrote the manuscript. Liang Hong also performed the experiment and analyzed the results.



A



B

Figure 1: Representative structures of (A) GFP and (B) CYP.

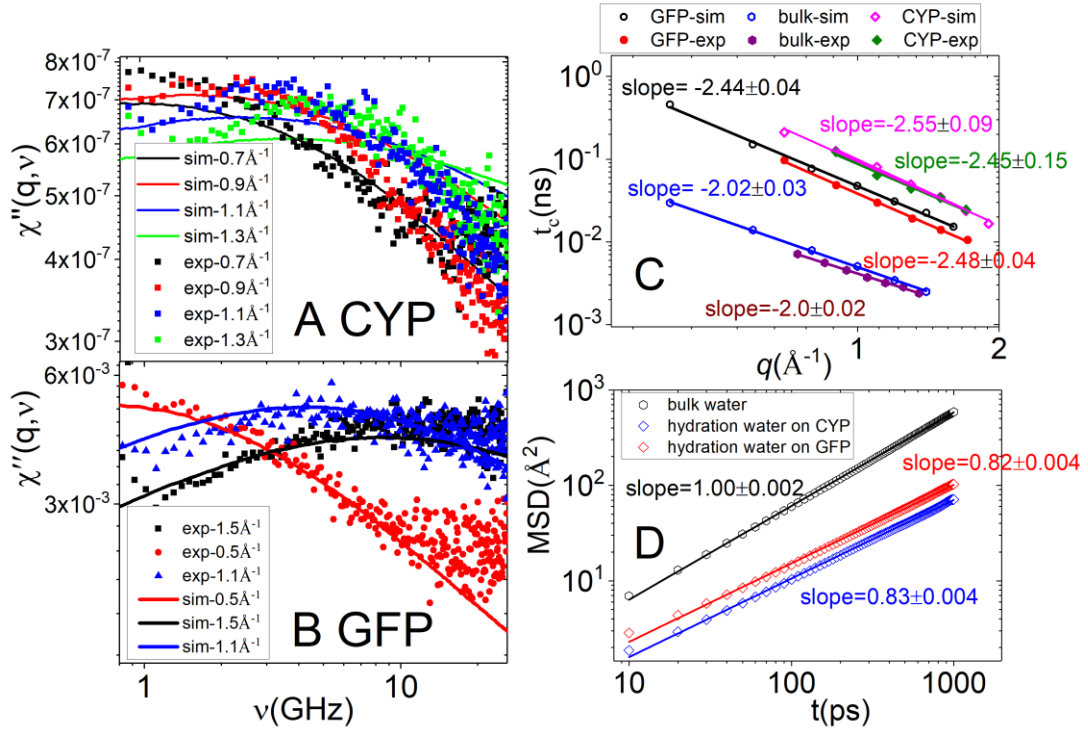


Figure 2: Neutron susceptibility spectra, $\chi''(q, \nu)$, for hydration water derived from experiment and from MD simulation on perdeuterated CYP (A) and GFP (B) [15] at various q values. More detailed experimental and simulation protocols can be found in SI. C: q dependence of the characteristic relaxation time, t_c , of hydration water and bulk water derived by fitting the χ'' spectra to the Cole-Cole function (Eq. (S2) in SI). Solid symbols represent experimental values while empty ones denote the MD-derived ones. Spheres denote hydration water on GFP, prisms correspond to hydration water on CYP and hexagons represent bulk water, where the experimental data of bulk water and hydration water on GFP were taken from Ref. [15]. D: the MD-derived MSD for both hydration and bulk water in the time window from 10 ps to 1 ns, black (bulk water), red

(hydration water in GFP) and blue (hydration water in CYP). Solid lines are power-law fits, with the exponents displayed accordingly.

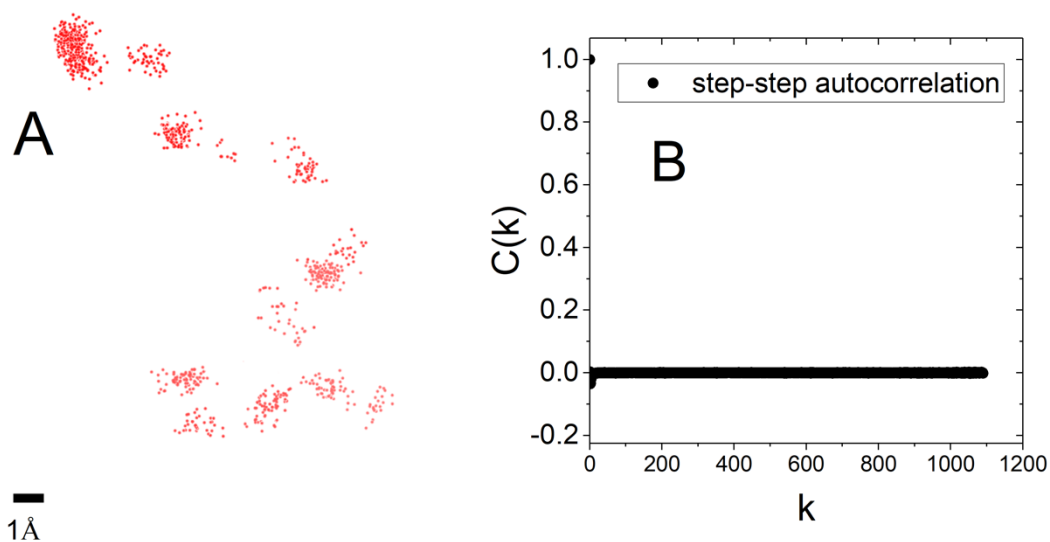


Figure 3: A: The projected MD trajectory of a selected water molecule on CYP. The position of oxygen atom of the water molecule is projected to a scatter plot at every 100 ps for a continuous trajectory of 100 ns long. B: The step-step auto correlation function of jump displacements, $C(k)$ (Eq. (1)) ensemble averaged over all the hydration water molecules on CYP. More example MD trajectory of water molecules on CYP and GFP are presented in Fig. S2 of SI. $C(K)$ derived for hydration water molecules on GFP is presented in Fig. S4B in SI.

CYP hydration water

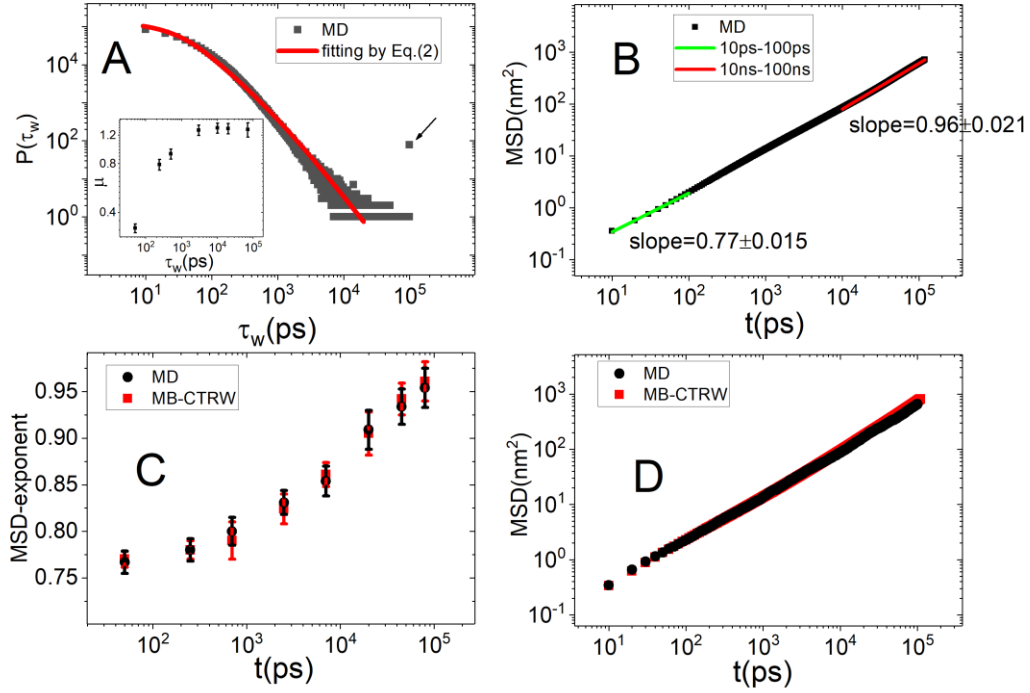


Figure 4: Statistical results derived for hydration water molecules on CYP. A: Black dots denote the distribution of waiting time, $P(\tau_w)$, derived directly from MD. The red curve represent a fit using Model MB-CTRW (Eq. (2)), yielding $\mu = 0.24157$, $\tau_0 = 10.362ps$ and $\eta=0.52172$. The arrow points out a small population of frozen water molecules ($\sim 1\%$ of the total water molecules), which are stuck in deep traps on the protein surface for the entire 100 ns MD simulation. The inset presents the dependence of the effective power law of $P(\tau_w)$ on the observation time, which is obtained by power-law fitting in one decay long time window. B: Mean square atomic displacement (MSD), $\langle X^2(\Delta t) \rangle$, derived from MD (black solid square). Green and red lines represent power-law fits in time window from 10ps to 100ps and from 10ns to 100ns respectively. C: Effective sub-diffusive exponent, β , obtained by performing power law fits to MSD derived from MD (black dots) and from Monte Carlo simulation based on MB-CTRW (red dots). Here, β is estimated by fits in different time windows, with each window being one decay long. D: MSD calculated directly from MD (black dots) and from Monte Carlo simulation based on Model MB-CTRW (red dots, see more details in SI).

GFP hydration water

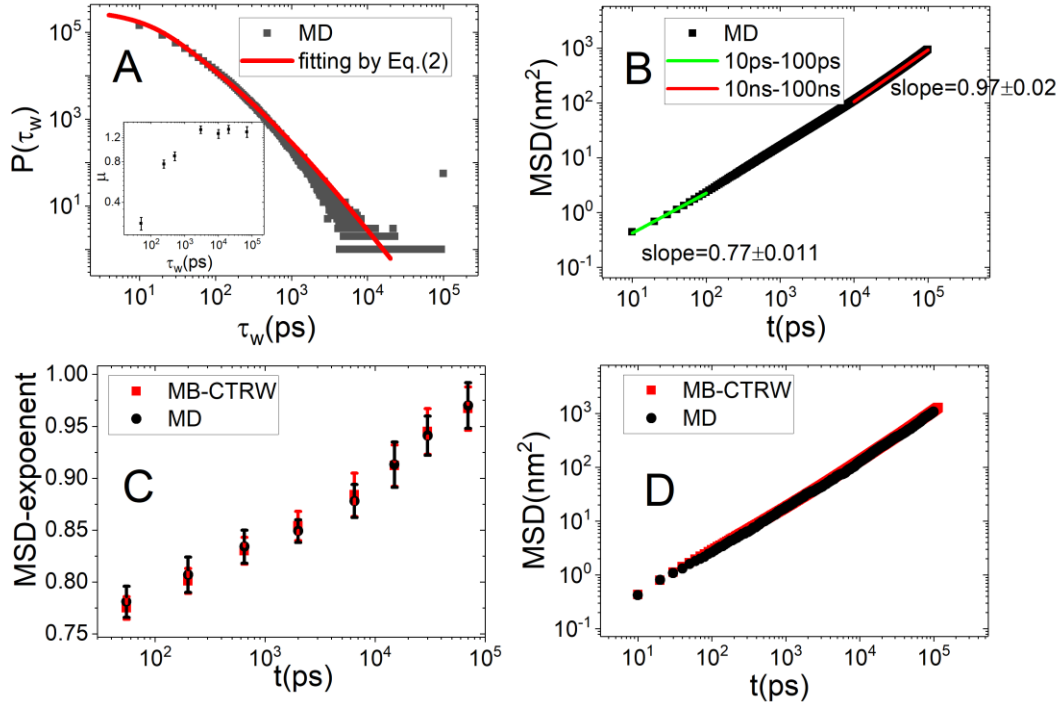


Figure 5: Statistical results derived for hydration water molecules on GFP. A: Black dots denote the distribution of waiting time, $P(\tau_w)$, derived directly from MD. The red curve represent a fit using Model MB-CTRW (Eq. (2)), yielding $\mu = 0.32167$, $\tau_0 = 8.3114ps$ and $\eta=0.49157$. The inset presents the dependence of the effective power law of $P(\tau_w)$ on the observation time, which is obtained by power-law fitting in one decay long time window. B: Mean square atomic displacement (MSD), $\langle X^2(\Delta t) \rangle$, derived from MD (black solid square). Green and red lines represent power-law fits in time window from 10ps to 100ps and from 10ns to 100ns respectively. C: Effective subdiffusive exponent, β , obtained by performing power law fits to MSD derived from MD (black dots) and from Monte Carlo simulation based on MB-CTRW (red dots). Here, β is estimated by fits in different time windows, with each window being one decays long. D: MSD calculated directly from MD (black dots) and from Monte Carlo simulation based on Model MB-CTRW

Reference

- [1] J. A. Rupley and G. Careri, in *Advances in protein chemistry* (Elsevier, 1991), pp. 37.
- [2] M. C. Bellissent-Funel, A. Hassanali, M. Havenith, R. Henchman, P. Pohl, F. Sterpone, D. Van Der Spoel, Y. Xu, and A. E. Garcia, *Chemical Reviews* **116**, 7673 (2016).
- [3] H. Frauenfelder, G. Chen, J. Berendzen, P. W. Fenimore, H. Jansson, B. H. McMahon, I. R. Stroe, J. Swenson, and R. D. Young, *Proceedings of the National Academy of Sciences* **106**, 5129 (2009).
- [4] B. Bagchi, *Chemical Reviews* **105**, 3197 (2005).

- [5] P. Ball, *Nature* **436**, 1084 (2005).
- [6] Y. Pocker, *Cellular and Molecular Life Sciences CMLS* **57**, 1008 (2000).
- [7] J. Payandeh, T. Scheuer, N. Zheng, and W. A. Catterall, *Nature* **475**, 353 (2011).
- [8] J. H. Roh, V. N. Novikov, R. B. Gregory, J. E. Curtis, Z. Chowdhuri, and A. P. Sokolov, *Physical Review Letters* **95**, 38101 (2005).
- [9] F. Merzel and J. C. Smith, *Proceedings of the National Academy of Sciences* **99**, 5378 (2002).
- [10] E. Duboué-Dijon, A. C. Fogarty, J. T. Hynes, and D. Laage, *Journal of the American Chemical Society* **138**, 7610 (2016).
- [11] S. Perticaroli *et al.*, *Journal of the American Chemical Society* **139**, 1098 (2016).
- [12] Y. von Hansen, S. Gekle, and R. R. Netz, *Physical review letters* **111**, 118103 (2013).
- [13] D. I. Svergun, S. Richard, M. H. J. Koch, Z. Sayers, S. Kuprin, and G. Zaccai, *Proceedings of the National Academy of Sciences* **95**, 2267 (1998).
- [14] S. Khodadadi, J. H. Roh, A. Kisliuk, E. Mamontov, M. Tyagi, S. A. Woodson, R. M. Briber, and A. P. Sokolov, *Biophysical journal* **98**, 1321 (2010).
- [15] J. D. Nickels *et al.*, *Biophysical Journal* **103**, 1566 (2012).
- [16] M. Settles and W. Doster, *Faraday Discussions* **103**, 269 (1996).
- [17] A. R. Bizzarri and S. Cannistraro, *The Journal of Physical Chemistry B* **106**, 6617 (2002).
- [18] A. R. Bizzarri, C. Rocchi, and S. Cannistraro, *Chemical physics letters* **263**, 559 (1996).
- [19] F. Pizzitutti, M. Marchi, F. Sterpone, and P. J. Rossky, *The Journal of Physical Chemistry B* **111**, 7584 (2007).
- [20] E. Mamontov, C. J. Burnham, S. H. Chen, A. P. Moravsky, C. K. Loong, N. R. De Souza, and A. I. Kolesnikov, *The Journal of chemical physics* **124**, 194703 (2006).
- [21] A. Faraone, K.-H. Liu, C.-Y. Mou, Y. Zhang, and S.-H. Chen, *The Journal of chemical physics* **130**, 134512 (2009).
- [22] E. Mamontov and K. W. Herwig, *Review of Scientific Instruments* **82**, 085109 (2011).
- [23] L. Hong, N. Smolin, B. Lindner, A. P. Sokolov, and J. C. Smith, *Physical review letters* **107**, 148102 (2011).
- [24] L. Hong, X. Cheng, D. C. Glass, and J. C. Smith, *Physical review letters* **108**, 238102 (2012).
- [25] L. Hong, N. Jain, X. Cheng, A. Bernal, M. Tyagi, and J. C. Smith, *Science advances* **2**, e1600886 (2016).
- [26] J. P. Bouchaud and A. Georges, *Phys. Rep.* **195**, 127 (1990).
- [27] X. Hu, L. Hong, M. D. Smith, T. Neusius, X. Cheng, and J. c Smith, *Nature Physics* **12**, 171 (2016).
- [28] Y. Meroz and I. M. Sokolov, *Physics Reports* **573**, 1 (2015).
- [29] Y. L. Miao, Z. Yi, D. C. Glass, L. Hong, M. Tyagi, J. Baudry, N. T. Jain, and J. C. Smith, *Journal of the American Chemical Society* **134**, 19576 (2012).
- [30] P. W. Fenimore, H. Frauenfelder, B. H. McMahon, and F. G. Parak, *Proceedings of the National Academy of Sciences* **99**, 16047 (2002).